GeoHazards

MDPI

Article

Seismicity Patterns in Some Mediterranean Zones After the 1939 Anatolian Earthquake: Insights on Seismic Risk and the Tectonic Setting

Enzo Mantovani [1], Marcello Viti [1,*], Caterina Tamburelli [1], Daniele Babbucci [1], Massimo Baglione [2] and Vittorio D'Intinosante [2]

[1] Dipartimento di Scienze Fisiche, Della Terra e Dell'ambiente, Università di Siena, 53100 Siena, Italy; enzo.mantovani@unisi.it (E.M.); tamburelli@unisi.it (C.T.); babbucci@unisi.it (D.B.)
[2] Regione Toscana, Settore Prevenzione Sismica, 50129 Firenze, Italy; massimo.baglione@regione.toscana.it (M.B.); vittorio.dintinosante@regione.toscana.it (V.D.)
* Correspondence: marcello.viti@unisi.it

Abstract: An attempt is made at recognizing the main effects of the strong 1939 earthquake in the Easternmost Anatolian Fault on the seismic activity in key Mediterranean tectonic zones. The major earthquake trends since 1800 indicate that, in the decades following 1939, both the number and intensity of significant earthquakes increased in the central and western NAF, the western Anatolia, the Crete–Rhodes Arc, the Peloponnesus, Sicily, and even the Tell zones. In contrast, seismicity experienced a sharp decline in the Serbo-Macedonian, Epirus-Albanides, and Calabria zones. These findings provide additional constraints on the geodynamic and tectonic framework and on the role played by post-seismic relaxation in the Mediterranean region.

Keywords: Anatolian earthquakes; post-seismic effects; Mediterranean tectonics

Received: 21 March 2025
Revised: 29 May 2025
Accepted: 3 June 2025
Published: 5 June 2025

Citation: Mantovani, E.; Viti, M.; Tamburelli, C.; Babbucci, D.; Baglione, M.; D'Intinosante, V. Seismicity Patterns in Some Mediterranean Zones After the 1939 Anatolian Earthquake: Insights on Seismic Risk and the Tectonic Setting. *GeoHazards* **2025**, *6*, 29. https://doi.org/10.3390/geohazards6020029

1. Introduction

In the long-term, tectonic activity in the Mediterranean region (Figure 1) is driven by the convergence of the Nubia and Eurasia plates and the westward extrusion of the Anatolian wedge (e.g., [1]). In the short-term, the effects of these kinematic boundary conditions are not continuous over time. They primarily develop after major earthquakes along the main fault systems. These events trigger perturbations in displacement, strain, and stress fields, which propagate through the surrounding regions at rates controlled by the elastic and viscoelastic properties of the crust and upper mantle [2–8]. The effects of these perturbations may be closely linked to the seismicity patterns of the zones involved. This study aims to identify the main effects of the strong earthquake (Mw = 7.7) that, in 1939, activated about 300 km of the eastern North Anatolian Fault (NAF) (e.g., [9–13]).

Several authors have suggested a close connection between the stress diffusion triggered by this event and the sequence of major earthquakes that occurred in the other segments of the NAF in the following decades, up to 1999 (Figure 2) (e.g., [8,14–16]).

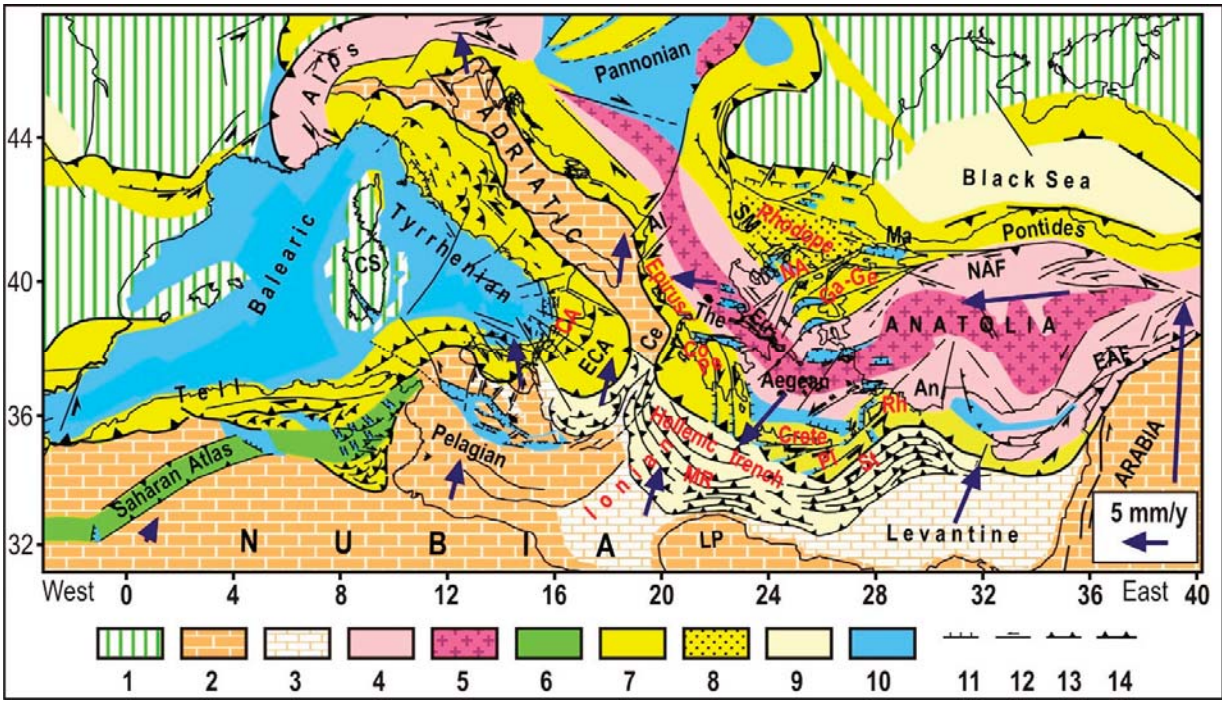

Figure 1. Tectonic scheme of the Mediterranean area. (1) European continental domain, (2) Nubia-Adriatic and Arabia continental domain, (3) Ionian-Levantine oceanic domain, (4, 5) outer and inner belts of the Tethyan system, constituted by metamorphic massifs and ophiolitic units, respectively, (6) Atlas belt, (7) other orogenic belts, (8) Rhodope and Serbo-Macedonian (SM) massifs, (9) Black Sea thinned domain, (10) Cenozoic basins, (11, 12, 13) extensional, transcurrent, and compressional features, and (14) outer fronts of the orogenic belts. Al = Albanides; An = Antalya peninsula; Ce = Cephalonia fault; Co = Corinth trough; CA = Calabria; CS = Corsica–Sardinia block; EAF = Eastern Anatolian Fault; ECA = External Calabrian Arc; Eu = Eubea; Ga-Ge = Ganos–Gelibolu thrust fault; Ma = Marmara trough; MR = Mediterranean ridge; NAF = North Anatolian Fault; NA = North Aegean trough; Pe = Peloponnesus wedge; Pl = Pliny fault; Rh = Rhodes; St = Strabo fault; The = Thessaly.

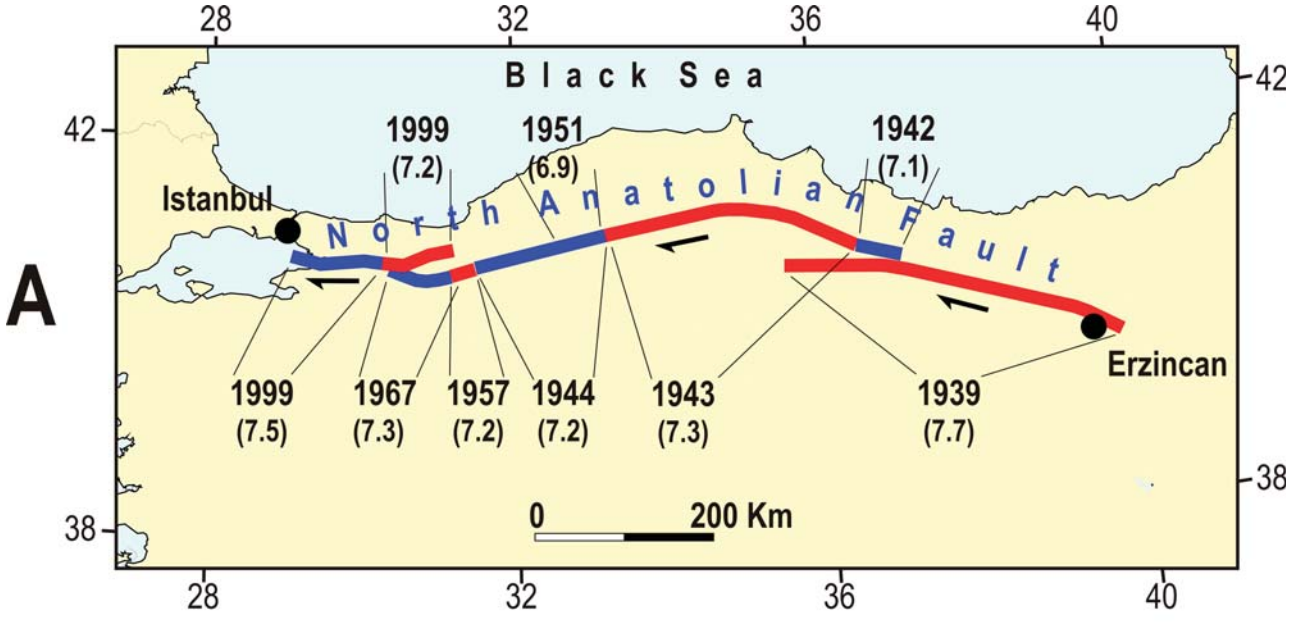

Figure 2. *Cont.*

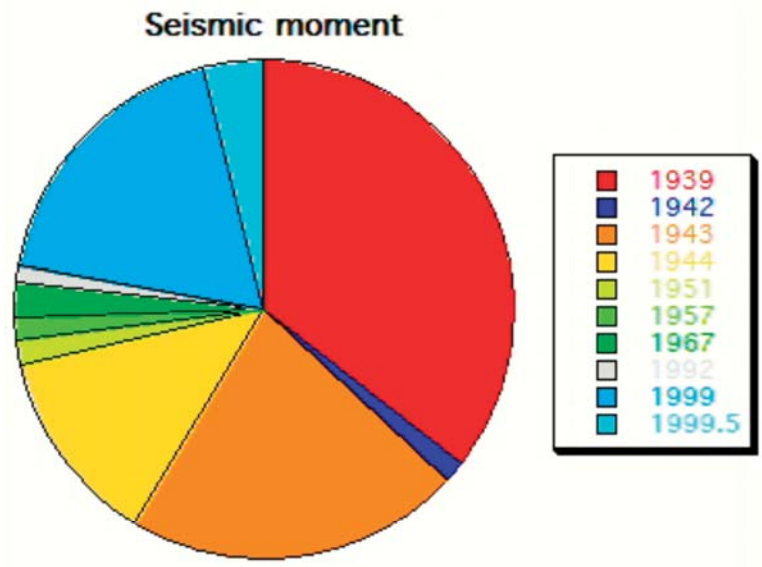

Figure 2. (**A**) Main segments of the North Anatolian Fault that failed since 1939 (based on [17,18]). Seismicity data as [19]. (**B**) The pie chart shows the relative seismic moment of the major earthquakes of the above sequence. The total seismic moment released from 1939 to 1999 is $1.16 \cdot 10^{21}$ Nm [15].

This seismic sequence caused a westward displacement of several meters (approximately 10) of the Anatolian wedge relative to the Black Sea domain (Figure 1; [9,10]). It is reasonable to expect that such a sudden and significant displacement of a major structure accelerated the deformation of zones directly or indirectly affected by Anatolia's motion. This primarily concerns the Aegean and Balkan sectors of the Tethyan system (Figure 1). Since these sectors (particularly their inner metamorphic core) transmit Anatolia's westward push to the Adriatic plate [1], which in turn exerts stress on the Pelagian domain and the northern Nubian margin [1,20–30], some effects of the 1939 Anatolian event can also be expected in the central and western Mediterranean regions.

2. Seismicity Time Patterns (1800–2024) and Underlying Tectonic Mechanisms

The seismic histories (since 1800) of the zones considered here are shown in Figure 3. For each zone some comments are reported about the main features of the seismicity time pattern, pointing out the main changes that occurred after 1939. Then, some hypotheses are advanced about the tectonic mechanisms that may be responsible for these changes.

2.1. North Anatolian Fault

The time pattern of seismic activity along this fault (Figure 3a, Table 1) shows a marked increase after the 1939 shock, mainly evident in the interval 1942–1967. This seismic sequence has been mainly attributed to the marked increase in shear stress that affected the central and western segments of the NAF after the strong 1939 event, as an effect of post-seismic relaxation (e.g., [3,4,8,10,15]).

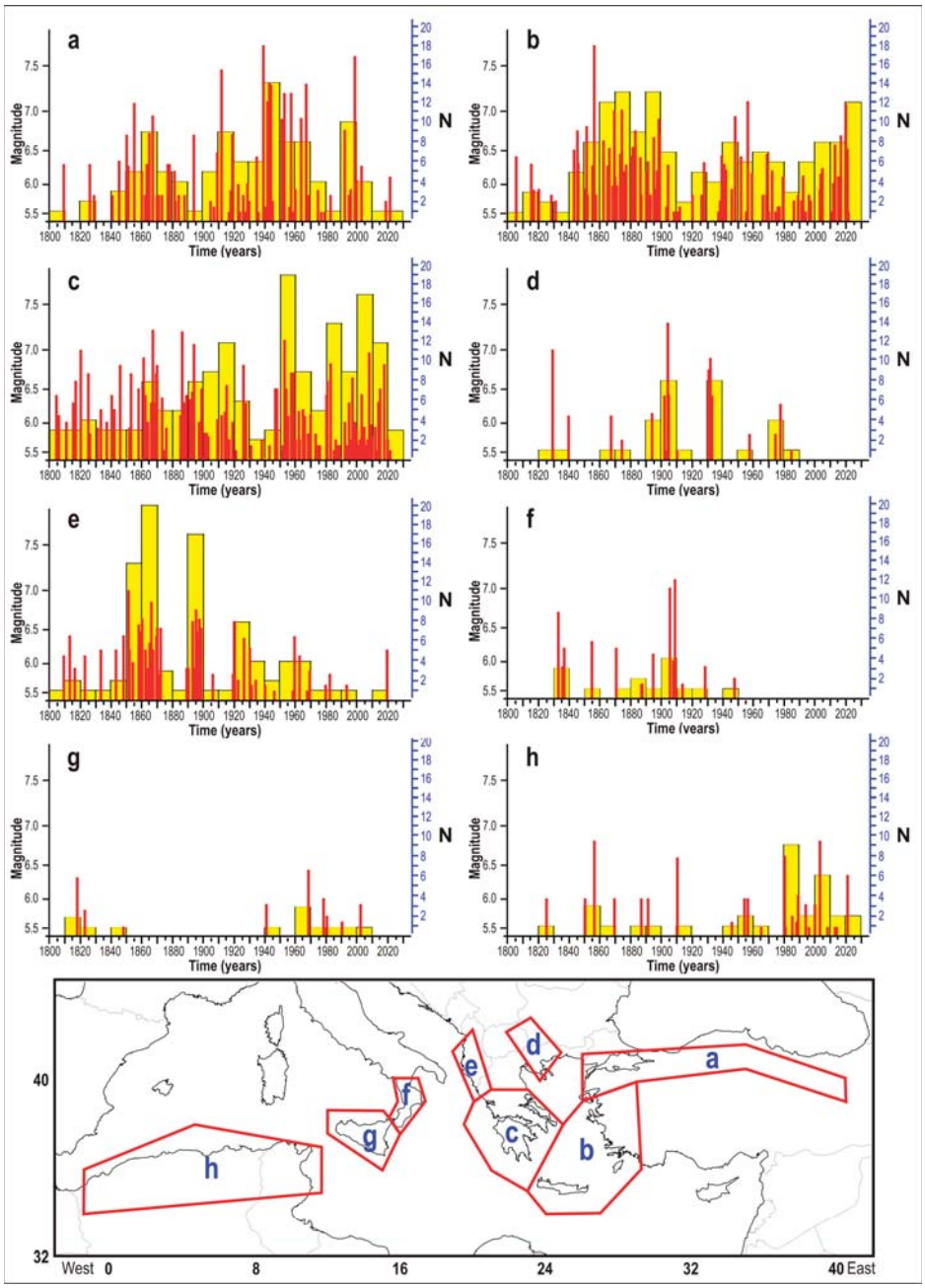

Figure 3. Time patterns of seismic activity since 1800. (**a**) North Anatolian Fault, (**b**) westernmost Anatolia and Crete–Rhodes arc, (**c**) southern Greece, (**d**) Serbo-Macedonian fault system, (**e**) Epirus thrust front and Albania shear faults, (**f**) Calabrian wedge, (**g**) Sicily, and (**h**) Tell belt. The yellow columns indicate the number of earthquakes with M ≥ 5.5, while the red bars relate to the equivalent magnitude (sum of energies converted in magnitude by the relation log E = 1.5M + 11.8) of the annual seismicity. The geometries of the zones considered are shown in the map, with the corresponding letters. Data from [19,31–41].

Table 1. Main earthquakes (M ≥ 5.5) that occurred since 1800 along the NAF (Figure 3a). The last column reports the numbers relating to the respective reference.

Year	M	R
1809	6.3	38
1826	6.3	38
1829	5.8	38

Table 1. *Cont.*

Year	M	R
1841	5.8	38
1845	5.8	38
1845	6.3	38
1850	6.7	38
1851	6.2	38
1851	5.8	38
1855	7.0	38
1855	6.7	38
1860	6.2	38
1862	5.8	38
1863	6.3	38
1865	6.4	38
1865	6.6	38
1867	6.9	38
1867	5.8	38
1867	5.8	38
1867	6.2	38
1870	5.8	38
1871	5.8	38
1873	5.8	19
1877	6.3	38
1878	6.3	38
1881	6.2	19
1882	5.7	38
1884	5.8	38
1888	5.8	19
1894	6.7	38
1905	5.7	36
1907	5.6	36
1909	6.4	19
1909	5.8	19
1909	5.8	19
1912	7.4	36
1912	6.2	36
1912	5.5	36
1912	6.9	36
1917	5.5	36
1918	5.8	19

Table 1. *Cont.*

Year	M	R
1918	5.5	19
1919	5.8	19
1919	6.7	36
1923	5.9	19
1923	5.6	36
1924	5.5	36
1926	5.8	36
1928	5.5	36
1929	6.0	19
1930	5.7	19
1935	6.2	36
1935	6.2	36
1936	5.5	19
1939	5.5	36
1939	7.7	19
1941	5.6	19
1942	5.7	36
1942	5.6	36
1942	5.5	19
1942	7.1	19
1943	6.4	36
1943	5.6	36
1943	7.3	19
1944	7.2	19
1944	5.5	19
1944	5.6	36
1944	5.6	19
1944	6.9	36
1945	5.7	19
1951	6.9	19
1953	7.2	36
1953	5.5	36
1953	5.5	36
1956	5.6	36
1957	5.9	36
1957	7.2	36
1959	5.5	36
1960	5.9	19
1964	5.7	36

Table 1. *Cont.*

Year	M	R
1964	6.9	36
1967	5.5	36
1967	7.3	36
1967	6.1	19
1967	5.7	36
1969	5.8	36
1975	5.5	36
1975	5.8	36
1977	5.5	19
1979	5.5	36
1983	5.8	36
1992	6.7	19
1992	6.3	19
1995	5.8	19
1996	5.7	19
1996	5.7	19
1999	7.5	36
1999	5.8	36
1999	5.6	36
1999	7.2	36
1999	5.5	36
2000	6	19
2000	5.5	36
2003	6.2	19
2003	5.8	36
2019	5.7	34
2022	6.1	34

2.2. Western Anatolia and Crete–Rhodes Arc

The highest seismic energy release occurred in the interval 1856–1900 (Figure 3b and Table 2). The fact that such crisis started just after the very strong shock that occurred in the Aegean zone in 1856 (M = 7.7) could not be casual. Then, seismicity was relatively low until 1948, when a new seismic phase occurred, involving two events with magnitudes 6.9 and 7.1 and a higher frequency of major events (Figure 3b). This phase, mainly developed during the interval 1948–1956, might be an effect of the post-1939 westward displacement of Anatolia. This hypothesis is suggested by the following considerations about the tectonic setting of the zones involved. The strain regime in the western Anatolian region mainly relates to S–N extension (e.g., [13,42,43]), which has developed since the early Pliocene (e.g., [44–46]). This regime may have been induced by a complex bending pattern of the Anatolian–Aegean Tethyan belt, which involves a NW-ward displacement of the northwestern sector and a SW-ward displacement of the southwestern sector (Figure 1). The consequent N–S extension between the above structures has been accommodated by the

formation of roughly E–W troughs. This tectonic mechanism and the related seismic activity may have been accelerated by the post-1939 westward displacement of Anatolia [23,25].

Table 2. Main earthquakes (M ≥ 5.5 that occurred since 1800 in the western Anatolian and Creta–Rhodes zones (Figure 3b).

Year	M	R
1805	6.4	38
1815	6.3	38
1817	5.8	38
1817	5.5	38
1820	5.9	38
1828	5.8	38
1831	5.7	38
1843	6.5	38
1845	6.7	38
1845	6.2	38
1846	6.1	38
1846	6.1	38
1850	5.9	38
1851	6.8	38
1852	5.8	38
1855	6.2	38
1855	5.8	38
1856	7.7	38
1856	6.1	38
1857	5.8	38
1862	6.3	38
1862	6.5	38
1865	5.8	38
1865	6.2	38
1866	5.8	38
1866	6.2	38
1866	6.1	38
1866	6.2	38
1868	5.8	38
1868	5.7	38
1869	6.8	38
1869	6.8	38
1870	6.1	38
1871	5.8	38
1871	5.7	38

Table 2. *Cont.*

Year	M	R
1873	5.9	38
1873	6.1	38
1873	6.2	38
1873	5.8	38
1874	7.0	38
1874	5.8	38
1875	5.8	38
1875	6.1	38
1877	6.2	38
1877	5.9	38
1880	6.2	38
1880	6.2	38
1881	6.5	38
1881	5.9	38
1883	6.7	38
1883	6.2	38
1886	6.3	38
1886	6.0	38
1887	5.8	38
1890	5.8	38
1890	6.1	38
1891	6.2	38
1891	5.9	38
1891	5.8	38
1892	5.8	38
1893	5.8	38
1895	6.6	38
1895	6.2	38
1896	5.9	38
1897	6.2	38
1898	6.9	38
1899	6.7	38
1903	5.6	36
1904	5.5	36
1904	6.0	36
1904	6.0	36
1904	5.8	36
1908	5.5	36
1909	5.5	36

Table 2. *Cont.*

Year	M	R
1910	5.5	36
1912	5.6	36
1920	5.8	36
1926	5.8	36
1927	5.6	36
1928	6.3	36
1928	5.6	36
1937	5.5	36
1938	5.7	36
1939	5.5	36
1939	6.4	36
1941	6.3	36
1942	5.5	36
1942	5.9	36
1942	5.5	36
1942	6	36
1946	5.9	36
1948	6.9	36
1948	6.2	36
1952	6.4	36
1955	5.5	36
1956	7.1	36
1956	6.0	36
1959	5.9	36
1959	6.0	36
1966	5.8	36
1968	5.8	36
1969	5.9	36
1969	5.9	36
1969	6.1	36
1969	5.9	36
1969	6.0	36
1970	5.5	36
1972	6.2	36
1974	5.5	36
1976	5.6	36
1977	5.6	36
1979	6.1	36
1986	5.7	36

Table 2. *Cont.*

Year	M	R
1989	5.6	36
1989	5.6	36
1991	5.7	36
1992	6	36
1992	5.8	36
1994	5.5	36
1996	5.8	36
1997	5.7	36
2003	5.8	36
2003	5.5	36
2004	6.1	36
2004	5.6	36
2005	5.6	36
2005	5.8	36
2005	5.8	36
2005	6.0	36
2011	5.5	35
2012	6.0	35
2013	6.2	35
2013	6.0	35
2013	6.4	35
2015	6.1	34
2017	6.3	34
2017	6.6	34
2020	5.6	34
2020	5.6	34
2020	5.7	34
2020	6.6	34
2020	5.8	34
2020	7.0	34
2021	5.5	34
2021	5.7	34
2021	6.0	34
2021	6.4	34
2021	5.6	34
2022	5.5	34

Seismotectonic activity in the Crete–Rhodes arc may be driven by the convergence between southwestern Anatolia (Antalya) and the Libyan promontory (Figure 1, [1,23–25]). The related shortening is accommodated by the southeastward bending and consequent

fragmentation of this arc. This tectonic mechanism also involves a sinistral relative motion between the Crete–Rhodes arc and the Levantine oceanic domain, which is accommodated by sinistral transpression at the Pliny and Strabo faults (Figure 1). The westward displacement of Anatolia after 1939 may have accelerated both the tectonic mechanisms cited above, causing the increase in seismic activity that mainly developed in the 1948–1956 interval (Table 2). The seismic crisis that has occurred in the last 20 years might be an effect of the two strong earthquakes (M = 7.5, 7.2) that hit the westernmost sector of the NAF in 1999.

2.3. Southern Greece (Peloponnesus, Cephalonia Fault, Corinth, Ambracique, Eubea, and Thessaly Troughs)

Two intense seismic crises developed in the 1860–1870 and 1886–1900 intervals (Figure 3c, Table 3). Then, activity significantly decreased until 1947, when a new intense seismic crisis started developing, involving major events until 1959, with 13 shocks of M $\geq$ 6 (seven with M $\geq$ 6.5). In the following period, seismicity decreased but never reached very low levels.

Table 3. Main earthquakes (M $\geq$ 5.5) that occurred since 1800 in southern Greece (Figure 3c).

Year	M	R
1804	6.4	38
1805	5.9	38
1806	6.1	38
1811	6.0	38
1815	6.3	38
1817	6.6	38
1820	6.6	38
1820	6.9	38
1825	6.7	38
1826	5.8	38
1831	5.9	38
1833	6.2	38
1837	6.0	38
1840	6.4	38
1842	6.2	38
1846	6.8	38
1852	5.9	38
1853	6.7	38
1858	6.5	38
1861	6.9	38
1862	6.4	38
1864	6.0	38
1866	6.3	38
1867	7.2	38
1867	6.5	38
1868	6.3	38

Table 3. *Cont.*

Year	M	R
1869	6.7	38
1870	6.8	38
1873	5.9	38
1873	6.3	38
1874	5.5	38
1876	5.9	38
1885	6.1	38
1886	7.2	38
1887	6.3	38
1888	6.3	38
1889	6.4	38
1891	6.3	38
1891	5.8	38
1893	6.3	38
1893	6.2	38
1894	6.8	38
1894	6.9	38
1897	6	38
1899	6.5	38
1901	5.5	36
1901	5.7	36
1902	5.7	36
1902	5.5	36
1903	5.6	36
1903	5.5	36
1909	5.9	36
1909	5.5	36
1909	5.6	36
1912	6.1	36
1914	5.9	36
1914	6	36
1915	6.1	36
1915	5.9	36
1915	6.3	36
1915	5.6	36
1915	6.0	36
1915	5.7	36
1916	5.7	36
1917	5.7	36

Table 3. *Cont.*

Year	M	R
1919	6.0	36
1921	5.5	36
1926	5.5	36
1926	5.7	36
1926	6.8	36
1927	5.6	36
1928	6.3	36
1931	5.6	36
1938	5.7	36
1943	5.6	36
1947	6.5	36
1948	6.5	36
1951	5.5	36
1952	5.6	36
1953	6.0	36
1953	6.6	36
1953	7.0	36
1953	5.9	36
1953	5.7	36
1953	6.1	36
1953	5.6	36
1953	6.2	36
1954	6.5	36
1955	6.0	36
1955	5.7	36
1957	5.9	36
1957	6.3	36
1957	6.6	36
1958	6.3	36
1959	6.7	36
1959	5.5	36
1960	5.7	36
1962	5.7	36
1962	6.1	36
1963	5.7	36
1965	6.2	36
1966	6.0	36
1966	5.7	36

Table 3. *Cont.*

Year	M	R
1968	5.8	36
1969	5.7	36
1970	6.0	36
1970	5.8	36
1973	5.8	36
1975	5.6	36
1976	5.6	36
1980	6.4	36
1981	6.4	36
1981	6.1	36
1981	6.2	36
1981	5.5	36
1981	5.6	36
1983	6.8	36
1983	5.5	36
1983	6.0	36
1985	5.5	36
1986	5.7	36
1987	5.5	36
1988	5.6	36
1989	5.6	36
1992	6.0	36
1994	5.6	36
1995	6.3	36
1996	5.7	36
1997	6.6	36
1997	5.6	36
1997	6.0	36
1998	5.6	36
1999	6.0	36
2000	5.8	36
2000	5.5	36
2001	5.6	36
2002	5.7	36
2003	6.4	36
2003	5.5	36
2005	5.8	36
2005	5.6	36

Table 3. *Cont.*

Year	M	R
2006	5.6	36
2007	5.7	35
2008	6.5	35
2008	6.8	35
2008	6.2	35
2008	6.4	35
2008	5.6	35
2009	5.7	37
2009	5.8	35
2010	5.5	35
2010	5.6	35
2012	5.8	35
2012	5.6	35
2013	5.5	35
2014	6.1	35
2014	6.1	35
2015	6.5	34
2018	5.5	34
2018	6.8	34
2018	5.6	34
2018	5.7	34
2020	5.7	34
2021	5.5	34
2022	5.5	34

We think that the increase in seismic activity since 1947 (Figure 3 and Table 3) may be an effect of the post-1939 Anatolian jump. This hypothesis is suggested by the fact that the post-1939 displacement of the Anatolian–Aegean system has induced a compressional regime in the Peloponnesus wedge. This regime has been accommodated by the south- to SW-ward escape of that wedge (e.g., [1,23–25,47,48]), guided by the dextral transpressional Cephalonia fault and by the system of curved shear faults that longitudinally cut the southern Peloponnesus. In turn, the roughly S–N divergence between the escaping Peloponnesus wedge and northern Greece has induced extensional stresses in the series of troughs located in central Greece (Corinth, Ambracique, Eubea, and Thessaly, e.g.,) as seen in Figure 1 [49–52].

2.4. Serbo-Macedonian Fault System (SM)

The time pattern of seismic activity in this zone shows a drastic drop in the period following 1939, highlighted by the fact that only one event (1978 M = 6.2) took place in this period, with respect to the previous interval (1800–1940), during which several shocks (14 with M > 6.0 and 5 with M > 6.5) took place (Figure 3d, Table 4). The hypothesis that such a decrease can be an effect of the post-1939 Anatolian advancement is supported by the fact that the push of Anatolia, transmitted by the Rhodope massif, induced a com-

pressional regime on the SM fault system, which may have inhibited the activation of the predominantly tensional faults recognized in that zone [1,23–25,53,54]. The compressional interaction between the northwestern Anatolian structure and the Rhodope massif is evidenced by the deformations observed in the interposed zone (Ganos–Gelibolu thrust zone, e.g., [55,56]) and by the earthquake focal mechanisms (e.g., the 1912 Ganos event [57,58]).

Table 4. Main earthquakes (M $\geq$ 5.5) that occurred since 1800 in the Serbo-Macedonian zone (Figure 3d).

Year	M	R
1829	7.0	38
1839	6.1	38
1867	6.1	38
1874	5.7	38
1894	5.8	38
1894	5.6	38
1894	5.9	38
1894	5.5	38
1902	6.4	36
1903	5.5	36
1904	7.2	36
1904	6.9	36
1904	6.3	36
1904	5.9	36
1905	6.4	36
1905	5.5	36
1910	5.5	36
1931	6.2	36
1931	6.7	36
1932	6.8	36
1932	6.0	36
1932	5.9	36
1932	6.4	36
1932	5.8	36
1933	6.4	36
1958	5.8	36
1975	5.8	36
1978	5.8	36
1978	6.2	36
1978	5.5	36
1985	5.5	36

The fact that the Serbo-Macedonian zone is experiencing a compressional regime is documented by geodetic observations carried out after the 1999 Izmit earthquake and by the uplift evidenced by neotectonic data [53,54]. One could wonder why in a zone periodically

stressed by the compressional perturbations induced by the advancements of Anatolia, the long-term (geological) data indicate a dominant extensional regime (e.g., [59–61]). This intriguing problem may find an explanation if one considers that this zone is also stressed by another driving force, whose effects dominate in the long-term with respect to the compressional ones produced by the advancements of Anatolia. The driving force of extension consists of the westward displacement of the northern Hellenides, which is driven by the push of the Aegean–Balkan Tethyan belt (Figure 1). This displacement may be triggered by the major seismic crises in the Epirus front, where the northern Hellenides overthrust the Adriatic plate (e.g., [25]) An important support to the above interpretation is given by the fact that the most intense shocks in SM (Figure 3d and Table 4) occurred during the most intense seismic phases in the Epirus–Albania (Figure 3e and Table 5).

Table 5. Main earthquakes (M $\geq$ 5.5) that occurred since 1800 in Epirus and Albanides (Figure 3e).

Year	M	R
1809	6.1	38
1813	6.4	38
1816	5.9	38
1823	6.1	38
1833	6.2	38
1843	6.2	38
1848	6.4	38
1851	6.8	38
1851	6.6	38
1851	6.4	38
1851	5.7	38
1851	5.9	38
1851	6.1	38
1852	6.2	38
1854	6.0	38
1858	5.9	38
1858	6.2	38
1858	6.4	38
1859	6.2	38
1859	5.9	38
1859	6.2	38
1860	6.4	38
1860	5.9	38
1860	6.2	38
1860	6.2	38
1862	6.2	38
1864	5.9	38

Table 5. *Cont.*

Year	M	R
1865	6.3	38
1866	6.6	38
1866	6.2	38
1866	5.9	38
1866	6.1	38
1866	5.9	38
1866	6.1	38
1866	5.9	38
1866	6.4	38
1867	6.2	38
1869	5.9	38
1869	5.5	38
1869	6.0	38
1869	6.2	38
1870	6.5	38
1871	5.8	38
1872	6.5	38
1889	5.9	38
1890	5.9	38
1893	6.6	38
1894	5.9	38
1895	6.2	38
1895	6.5	38
1895	6.2	38
1895	6.2	38
1895	6.2	38
1896	5.9	38
1896	6.2	38
1896	5.9	38
1896	5.9	38
1896	5.9	38
1897	6.6	38
1897	5.7	38
1897	5.7	38
1898	6.5	38
1906	5.8	36
1919	5.8	36

Table 5. *Cont.*

Year	M	R
1920	5.6	36
1920	6.5	36
1920	5.9	36
1920	6.0	36
1920	5.7	36
1922	5.7	36
1926	5.9	36
1926	6.3	36
1930	6.2	36
1930	5.5	36
1931	5.6	36
1934	5.7	36
1940	5.6	36
1946	5.5	36
1958	5.5	36
1959	5.9	36
1959	6.3	36
1959	5.7	36
1962	6.1	36
1967	5.5	36
1969	5.7	36
1969	5.6	36
1979	5.6	36
1982	5.8	36
1993	5.6	36
2019	6.2	39

2.5. Outer Northern Hellenides (Epirus) and Albanides

During the 1800–1930 time-interval, these zones were affected by many major ($M \geq 6$) earthquakes (Figure 3e, Table 5), including ten shocks with $M \geq 6.5$. Then, this activity underwent a considerable drop from 1931, only involving three earthquakes with $6 \leq M \leq 6.5$. in more than 90 years.

A possible explanation for this drastic drop of seismicity may be found by considering some major aspects of the tectonic context. During the periods of low activity along the NAF and EAF, seismotectonic activity in the Epirus thrust front is mostly due to the convergence between the Adria plate (moving roughly NNE-ward, in connection with Nubia) and the northern Hellenides. After major seismic sequences along the NAF, such as the one that occurred since 1939, the westward push of the Anatolian–Aegean Tethyan system, transmitted by the Peloponnesus wedge, may cause a slowdown accompanied by an upward flexure of the southernmost Adriatic–Ionian domain. This induces an attenuation of the compressional regime in the Epirus thrust front (and of the related seismic activity). The same mechanism could have reduced the right lateral motion between the northern

Hellenides and the southern Dinarides, decreasing shear stress (and seismicity) at the decoupling transpressional faults in the Albanides (Figure 1).

2.6. Calabrian Wedge

This zone (Figure 3f, Table 6) has not been affected by major earthquakes (M ≥ 5.5) since 1948. Such a long quiescence (77 years) can be considered as an anomalous "seismic behavior" of Calabria, given that the time lengths of the previous quiescences (since 1600) were never longer than 49 years and that the average inter-event time in the interval 1600–1948 is about 12 years (Table 6).

Table 6. Main earthquakes (M ≥ 5.5) that occurred since 1600 in the Calabrian wedge.

Year	M	R
1609	5.8	40
1626	6.1	40
1638	7.1	40
1638	6.8	40
1640	5.8	40
1659	6.6	40
1708	5.6	40
1743	5.9	40
1744	5.7	40
1749	5.8	40
1767	5.9	40
1783	7.1	40
1783	6.7	40
1783	7	40
1791	6.1	40
1832	6.7	40
1835	5.9	40
1836	6.2	40
1854	6.3	40
1870	6.2	40
1886	5.6	40
1887	5.6	40
1894	6.1	40
1905	7	40
1907	6	40
1908	7.1	40
1909	5.5	40
1913	5.6	40
1928	5.9	40
1947	5.7	40

We suggest that the seismic quiescence of this zone since 1948 may be an effect of the upward flexure and slowdown that the southern Adria plate has undergone in response to the westward push of the Anatolian–Aegean Tethyan system. Such deformation may have significantly increased the resistance against the overthrusting of the Calabria wedge on the Ionian domain, i.e., the tectonic process that is mainly responsible for seismic activity in that fragmented wedge.

2.7. Sicily

Seismic activity in this zone has been very low for a long time-interval (1800–1967), during which only five earthquakes with $5.5 \leq M \leq 6.5$ have occurred (Figure 3g and Table 7). The number of these events significantly increased in the following period, when seven shocks with $M \geq 5.5$ took place in about 50 years. The possibility that the seismic behavior of Sicily in recent decades can be considered "anomalous" is also suggested by what happened in the previous two centuries (Table 7), during which the magnitude of earthquakes overcame the value of six in only three cases (1693 M = 6.1, 7.3; 1786 M = 6.1) and the average inter-event time was about 25 years, which is almost double the one in the 1968–2024 interval.

Table 7. Main earthquakes ($M \geq 5.5$) that have occurred since 1600 in Sicily.

Year	M	R
1613	5.6	40
1624	5.6	40
1693	6.1	40
1693	7.3	40
1698	5.7	40
1726	5.5	40
1780	5.5	40
1786	6.1	40
1818	6.3	40
1818	5.6	40
1823	5.8	40
1848	5.5	40
1941	5.9	40
1968	6.4	40
1968	5.5	40
1968	5.5	40
1978	6	40
1980	5.7	40
1990	5.6	40
2002	5.9	40

To understand the tectonic mechanism that may have caused the above increase in seismicity it is necessary to consider the tectonic evolution of this zone, that since the early Pliocene was driven by the westward push of the Anatolian–Aegean Tethyan system (Figure 4 [1,22,25–27]). This mechanism caused the decoupling of the Adriatic plate from Nubia through the formation of a long discontinuity crossing the Ionian domain (Victor

Hensen–Medina fault) and the Hyblean–Pelagian domain (Sicily Channel fault system). Once decoupled, the Adria plate underwent a clockwise rotation, inducing a strong E–W compression on the Hyblean–Pelagian domain (Figure 4B). The consequent shortening was accommodated by the northward escape of the Adventure block and of the adjacent Maghrebian sector. In turn, the indentation of these structures induced the lateral escape of Alpine–Apennine wedges (southern Apennines and Calabria), with the formation of the central (Vavilov) and southern (Marsili) Tyrrhenian basins. A detailed explanation of this evolution is reported by [1,22,30].

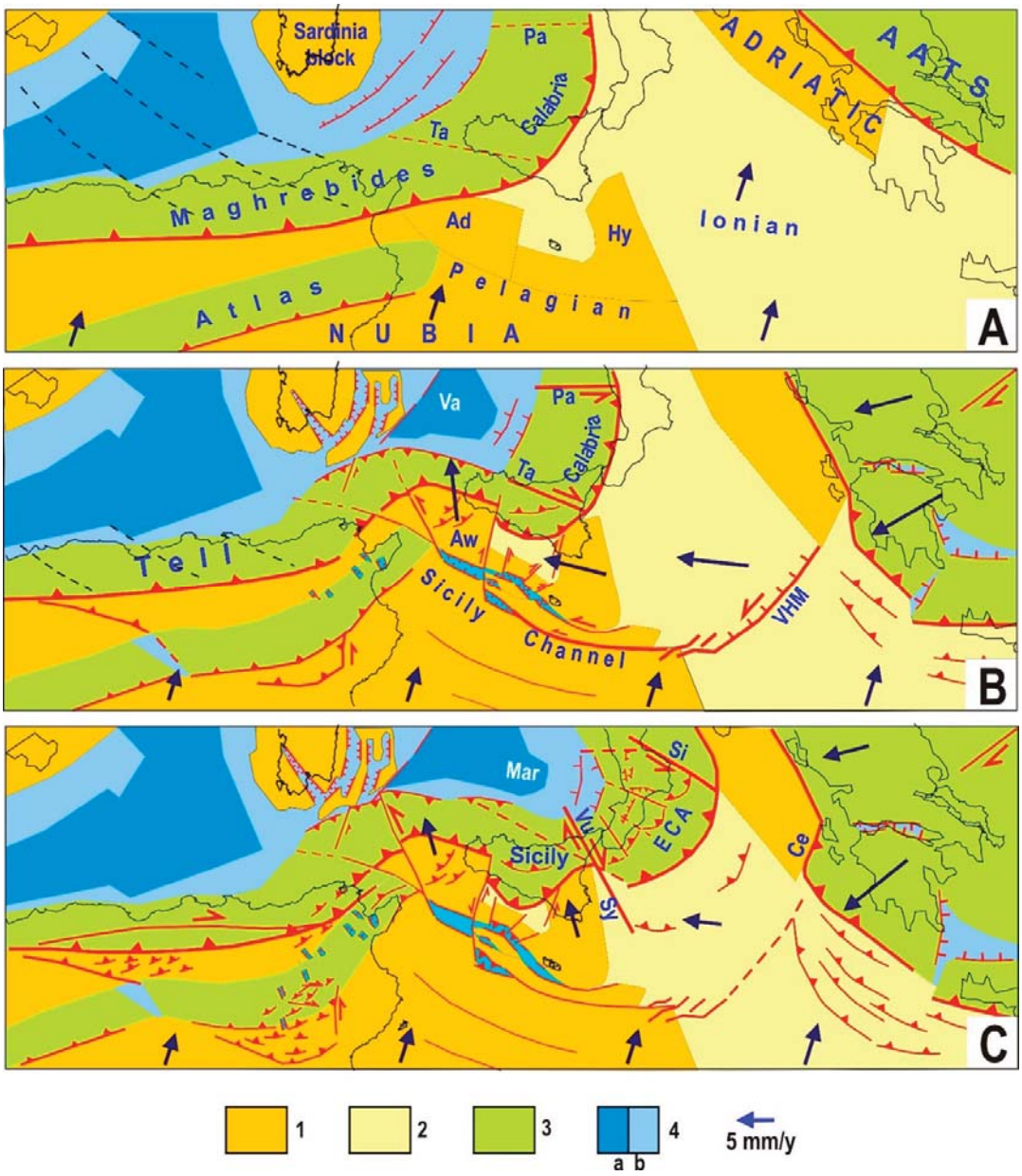

Figure 4. Tentative reconstruction of the tectonic processes that developed in the central and western Mediterranean regions in response to the late Miocene collision between the Anatolian–Aegean Tethyan system (AATS) and the Adriatic promontory [1]. See text for explanations. (1) Continental domains, (2) thinned continental and oceanic domains, (3) orogenic belts, and (4) zones of intense (a) or moderate (b) crustal thinning. (**A**) Late Miocene. Ad = Adventure domain; Hy = Hyblean plateau, Pa = Palinuro fault, and Ta = Taormina fault. (**B**) Middle Pliocene. Aw = Adventure wedge, Va = Vavilov basin, and VHM = Victor Hensen–Medina fault. (**C**) Middle Pleistocene. Ce = Cephalonia fault, ECA = External Calabrian Arc, Mar = Marsili basin, Si = Sibari fault, and Sy-Vu = Syracuse–Vulcano fault. Other symbols as in Figure 1.

Around the late Pliocene–early Pleistocene, the collision of the northern Calabrian wedge with the continental Adriatic domain caused an important change in the tectonic setting of this zone, involving a different escape trend of Calabria and the activation of the Vulcano–Syracuse fault system (Figure 4C [1]). This last discontinuity has promoted the roughly northward escape of the Hyblean block, inducing a compressional regime along its northern margin, offshore of northern Sicily [62,63]. These tectonics are still going on and may be responsible for the thrusting indicated by neotectonic data and earthquake focal mechanisms [64,65]. The acceleration of E–W compression, driven by the post-1939 Anatolian jump, may explain why the average inter-event time in Sicily has considerably decreased in recent decades (Figure 3g and Table 7).

2.8. Tell System

The time pattern of major earthquakes ($M \geq 5.5$, Figure 3h, Table 8) shows an evident increase in recent decades (perhaps since 1954 and more evidently since 1980), highlighted by the high number of shocks (yellow bands in Figure 3h) and by the fact that in about 40 years this zone was hit by six earthquakes with $M \geq 6$ and two with $M \geq 6.5$ (Table 8). In the previous much longer interval (1800–1979), only two shocks reached a magnitude greater than six.

Table 8. Main earthquakes ($M \geq 5.5$) that have occurred since 1800 in the Tell (Figure 3h).

Year	M	R
1825	6.0	32
1850	6.0	32
1856	6.0	31
1856	6.8	31
1869	6.0	32
1887	6.0	32
1891	6.0	32
1910	6.6	33
1946	5.6	32
1954	6.0	33
1956	6.0	33
1965	5.5	33
1980	6.5	41
1980	5.9	41
1980	6.2	41
1980	5.7	33
1981	5.5	41
1985	5.7	33
1988	5.6	33
1989	6.0	41
1989	5.5	33
1994	5.9	35

Table 8. *Cont.*

Year	M	R
1996	5.5	35
2000	5.7	35
2000	5.7	35
2003	6.8	41
2003	5.7	41
2003	5.7	35
2008	5.5	35
2013	5.5	35
2014	5.5	34
2021	6.2	39
2021	6.1	39

As suggested by [25–27], seismotectonic activity in the northern Nubian margin is influenced by the westward displacements of Anatolia. The push of this large wedge, transmitted by the Aegean arc and the Adria–Pelagian domain, induces E–W compression in the northern Nubian margin. This regime, combined with the NE-ward compression driven by the Nubia–Eurasia convergence, induces the dextral transpressional shear in the Tell which is indicated by neotectonic and seismological data. This tectonic context may explain the increase in seismic activity that occurred in this zone in recent decades, when the effects of the Anatolian jump might have stressed the Tell.

3. Discussion

This study suggests that the peculiar distribution of seismicity temporal patterns following the 1939 Great Anatolian Earthquake aligns with the tectonic implications of the geodynamic context proposed by the authors of [1,24,25]. Since the relevant literature presents alternative interpretations involving different driving forces and tectonic processes, it is useful to assess how these perspectives explain the evidence discussed here.

As an example, we highlight the challenges of adopting the well-known idea that Plio–Quaternary deformation in the Mediterranean region has been primarily driven by the gravitational sinking of subducted lithospheres (slab-pull model; e.g., [66–72]). This model implies that tectonic activity in the eastern Mediterranean is mainly governed by the southwestward pull of the retreating Ionian–Levantine slab. However, in such a scenario, the post-1939 westward displacement of Anatolia would have counteracted rather than accelerated the extensional effects of slab-pull in the Aegean region, leading to a decrease in seismicity rather than an increase.

One of the primary arguments supporting the slab-pull model (e.g., [73] is the observation that geodetic velocities in the Aegean region (30–40 mm/yr) are significantly higher than those in Anatolia (10–15 mm/yr). However, this interpretation does not consider that the current velocity field could represent a transient condition resulting from post-seismic viscoelastic relaxation triggered by the post-1939 Anatolian seismic sequence (e.g., [74–76] and references therein).

Another piece of geodetic evidence cited in support of the hypothesis that Anatolia is being pulled (by slab-pull) rather than pushed (by the indentation of Arabia) comes from the analysis of coseismic and postseismic displacement fields induced by the two strong earthquakes (M = 7.6, 7.8) that struck the Eastern Anatolian Fault in February 2023 [77].

The evidence that is supposed to demonstrate the above hypothesis is based on the fact that no present-day shortening is indicated by the observed geodetic deformation field at the Arabia–Anatolia boundary. However, this interpretation does not take into account that the 2023 activations of the Eastern Anatolian Fault occurred after the very strong seismic sequence that has developed along the NAF since 1939. These breaks allowed a large westward displacement of the northern Anatolian structure, causing it to diverge from southeastern Anatolia (which was less mobilized), thereby inducing a NW–SE extensional stress field at the EAF system. This suggests that the 2023 activations of that fault may have released the extensional strain previously accumulated.

The hypothesis that the westward motion of Anatolia is driven by a pull (such as the retreat of the Aegean slab) rather than by the indentation of Arabia struggles to account for other major features. The most evident is the shape of the Anatolian–Aegean Tethyan belt (Figure 1), which testifies a considerable bending. This compressional deformation is clearly incompatible with a westward pull. Another major feature that the slab-pull model struggles to explain is the presence of an extensional zone (Cretan basins) between the presumed driving force (Hellenic slab pull) and the Anatolian wedge. Additionally, it would be necessary to explain why the eastern and western Cretan basins developed at rather different times (e.g., [78,79]). Other significant inconsistencies between the observed deformation pattern and the implications of the slab-pull model are discussed by the authors of [1,23–25,30].

The slab-pull model also implies that tectonic activity in the central and western Mediterranean regions is not significantly influenced by the extrusion of Anatolia. However, this assumption makes it difficult to explain why after the 1939 Anatolian shock seismicity increased in Sicily and in the Tell and decreased in the Epirus–Albania and Calabria.

Another key difference between the geodynamic interpretation adopted here and the alternative ones concerns the direction of the Nubia–Eurasia convergence, which is often assumed to be oriented towards the northwest (e.g., [73,80–83]). This trend is difficult to reconcile with several important pieces of evidence from across the Mediterranean region (e.g., [1] and references therein [20]). The main difficulty lies in explaining how the Adria plate can move in an approximately perpendicular direction (towards the NNE [84,85]), despite no significant active decoupling between Nubia and Adria being recognized ([1] and references therein). A detailed discussion of these issues can be found in [1,20,22,23,29,30,86].

Several modeling studies have attempted to reproduce the effects of the post-seismic relaxation triggered by major shocks in the study area (e.g., [3,4,8,75,87]. However, the results indicate a wide range of possible effects. This variability is mainly due to insufficient knowledge of the actual structural and rheological parameters, which allows researchers to adopt different models involving the various layering of elastic and viscoelastic properties, as well as different boundary conditions. Because of this uncertainty, the results of these studies may be affected by unknown errors, making them unreliable for seismic hazard assessments. In this regard, we believe that useful insights into seismic hazards can be obtained by studying the spatio-temporal distribution of seismicity following strong shocks, and by the attempts to understand their possible connection with the geodynamic frameworks and the ongoing tectonic processes.

4. Conclusions

The post-1800 time patterns of seismic activity in key tectonic zones of the Mediterranean area suggest that the seismic sequence that has activated the whole North Anatolian Fault since 1939, has also accelerated the ongoing tectonic processes in western Anatolia, the eastern (Crete–Rhodes) and western (Peloponnesus) Hellenic arcs, Sicily, and northern

Nubia, and decelerated deformations in the Serbo-Macedonian, Albanian, Epirus, and Calabrian zones. In the Aegean zones, the increase in seismicity may be due to fact that the westward displacement of Anatolia has accelerated the southward bending of the Aegean metamorphic core, leading to the fragmentation of the surrounding brittle orogenic structures. This process may have induced S–N extension in the westernmost Anatolia, NE–SW shortening in the Crete–Rhodes arc, NNE–SSW escape of the Peloponnesus wedge, and N–S extension in the Corinth, Ambracique, Eubea, and Thessaly troughs. The fact that no major shocks have occurred in the Serbo-Macedonian tensional fault system since about 1932 might be a consequence of the post-1939 compressional regime induced by the westward push of northern Anatolia, transmitted by the Rhodope massif.

The drastic drop in seismicity in the Epirus–Albania zone since about 1967 (following a long period of high activity) may indicate that the tectonic mechanism responsible for seismic activity at this thrust front (namely the convergence between the southern Adria domain and the northern Hellenides) has slowed down after the 1939 event. This effect may have been caused by the upward flexure and deceleration of the southernmost Adriatic domain in response to the westward push of the Anatolian–Aegean system. A temporary deformation of the southern Adria domain could also explain the absence of major earthquakes in Calabria since 1948, as such upward flexure may have increased the resistance against the outward migration of the Calabrian wedge, which is the mechanism primarily responsible for the breaking of that wedge. Moreover, the increase in seismic activity in Sicily after 1940 might have been the result of an acceleration of the northward motion of the Hyblean block in response to the westward push of the Anatolian–Aegean system. This driving force may also explain the increased seismic activity observed in the Tell region (e.g., [1,25–27]).

One could try a quantification of the statistical significance of the increases and decreases tentatively identified in the zones considered. However, we think that such information would be scarcely useful. In this regard, it can be pointed out that the variations in seismicity in the considered zone have occurred some decades after the 1939 event, which is within a range of time-intervals which are compatible with the migration rates of the post-seismic relaxation triggered by the Anatolian seismic sequence. Moreover, it can be pointed out that the increases and decreases in seismicity well-correspond to the implications of the tectonic setting in the respective zones. The possibility that such complete correspondence can merely occur by chance is certainly very low. We believe that the information provided by this work about the seismicity patterns that occurred in key tectonic zones after the strong 1939 earthquake may be useful for any study of seismic risk in the zones involved. The reader will use this information in the way they think to be plausible.

The evidence and arguments presented in this work may enhance our understanding of the relationship between the short-term development of ongoing tectonic processes and the spatiotemporal distribution of major earthquakes in the Mediterranean region. This knowledge could be useful for identifying the zones most prone to significant seismic events in the coming decades. To explain this proposal more clearly, we present some possible examples.

- After the considerable stress drops that occurred in the North Anatolian Fault (NAF) during previous decades, one might assume that the shear stress along this discontinuity has significantly decreased, potentially implying a moderate risk of major events. However, this tentative prediction may not apply to the easternmost sector of the NAF, as the two strong earthquakes that struck the Eastern Anatolian Fault in 2023 (M = 7.8, 7.6) may have facilitated a westward displacement of the easternmost Anatolian wedge, thereby increasing shear stress along the easternmost segment of

the NAF. Nevertheless, it is unlikely that such an increase could fully reload the fault near the rupture point, given the significant drop in stress in 1939. We believe that a geodetic analysis of the strain field evolution in these areas can be useful.

- The progressive decrease in seismic activity following the intense seismic phase between 1948 and 1960 (Figure 3, Table 2) could indicate that the effects of the major Anatolian displacement in the western margin of Anatolia have passed their most intense phase. However, the emergence of a new seismic phase around 2013, which includes nine earthquakes with $M \geq 6$, may suggest that this fault system is experiencing a stress increase, possibly triggered by the two strong earthquakes that occurred in 1999 along the westernmost NAF (Marmara Sea region, M = 7.5, 7.2). The recent seismic activity in the Santorini region and its potential developments could be part of this ongoing seismic phase.
- One could expect that the two strong earthquakes that in 1999 hit the westernmost sector of the NAF have also triggered an increase in shear stress in the North Aegean Faults located along the two-branches westward of the NAF. This hypothesis is compatible with the occurrence of a major shock (M = 6.9) in 2014 along the above zone.
- The compressional effects induced by the post-1939 Anatolian jump (documented by geodetic data) and the seismic quiescence in the Epirus zone since 1940 suggest a low hazard in the normal faults of the Serbo-Macedonian zone, as argued earlier.
- The seismic history of southern Greece shows almost continuous activity in the last two centuries. This evidence, corroborated by the fact that three major shocks have recently occurred in Cephalonia fault in 2018, M = 6.8, and in the Thessaly troughs in 2021, M = 6.3 and 6.2, does not allow us to exclude the occurrence of a major shock in the next decade.
- In the Epirus–Albanides zone, the lack of major earthquakes during a relatively long period (1963–2002) might be an effect of the deformation that the southern Adria plate is undergoing in response to the westward push of the Anatolian–Aegean system. However, the occurrence of some significant shocks in the last 20 years (2003 M = 6.4, 2015 M = 6.5, and 2019 M = 6.2) could indicate the progressive mitigation of the above effect, with a consequent progressive increase in seismic hazard.
- In Calabria, the complete absence of events with $M > 5.5$ since 1947 may lead us to suppose that the present seismic hazard is not high. However, it is not easy to recognize how long this situation can go on for. The analysis of geodetic data may help to recognize eventual changes in the velocity field, possibly induced by the attenuation of the effects of the post-1939 Anatolian jump.
- The fact that geodetic data indicates a roughly NW-ward motion of the northern Nubian belt (in contrast to the NNE-ward trend inferred from the Plio–Quaternary deformation pattern [1,26,27]) suggests that this zone is still experiencing the effects of the Anatolian jump and that consequently the occurrence of major shocks in the next decade can hardly be excluded.

Author Contributions: Conceptualization and methodology E.M. and M.V.; Investigation and data curation E.M., M.V., D.B., C.T., M.B. and V.D.; Writing E.M.; Fund acquisition: E.M., M.B. and V.D. All authors have read and agreed to the published version of the manuscript.

Funding: This research was funded by the Regione Toscana (Italy), Department of Seismic Prevention, grant number: B65F19003190002.

Data Availability Statement: This information was reported by the cited references.

Conflicts of Interest: The authors declare no conflict of interest.

References

1. Mantovani, E.; Viti, M.; Babbucci, D.; Tamburelli, C. *Neogenic Evolution of the Mediterranean Region: Geodynamics, Tectonics and Seismicity*; Springer Nature: Cham, Switzerland, 2024; p. 174. ISBN 3031621492/9783031621499.
2. Anderson, D.L. Accelerated plate tectonics. *Science* **1975**, *167*, 1077–1079. [CrossRef]
3. Mantovani, E.; Viti, M.; Cenni, N.; Albarello, D.; Babbucci, D. Short and long-term deformation patterns in the Aegean-Anatolian systems: Insights from space geodetic data (GPS). *Geophys. Res. Lett.* **2001**, *28*, 2325–2328. [CrossRef]
4. Cenni, N.; D'onza, F.; Viti, M.; Mantovani, E.; Albarello, D.; Babbucci, D. Post seismic relaxation processes in the Aegean-Anatolian system: Insights from space geodetic data (GPS) and geological/geophysical evidence. *Boll. Geofis. Teor. Appl.* **2002**, *43*, 23–36.
5. Kenner, S.; Segall, P. Lower Crustal Structure in Northern California: Implications From Strain-Rate Variations Following the 1906 San Francisco Earthquake. *J. Geophys. Res.* **2003**, *108*, ETG 5-1–ETG 5-17. [CrossRef]
6. Freed, A.M.; Bürgmann, R. Evidence of power-law flow in the Mojave Desert mantle. *Nature* **2004**, *430*, 548–551. [CrossRef] [PubMed]
7. Freed, A.M. Earthquake triggering by static, dynamic, and postseismic stress transfer. *Annu. Rev. Earth Planet. Sci.* **2005**, *33*, 335–367. [CrossRef]
8. Sunbul, F.; Nalbant, S.S.; Simão, N.M.; Steacy, S. Investigating viscoelastic postseismic deformation due to large earthquakes in East Anatolia, Turkey. *J. Geodyn.* **2016**, *94–95*, 50–58. [CrossRef]
9. Barka, A.A. Slip distribution along the North Atlantic fault associated with the large earthquakes of the period 1939 to 1967. *Bull. Seismol. Soc. Am.* **1996**, *86*, 1238–1254. [CrossRef]
10. Stein, R.S.; Barka, A.A.; Dieterich, J.H. Progressive failure on the North Anatolian fault since 1939 by earthquake stress triggering. *Geophys. J. Int.* **1997**, *128*, 594–604. [CrossRef]
11. Şengör, A.M.C.; Tüysüz, O.; İmren, C.; Sakınç, M.; Eyidoğan, H.; Görü, N.; Le Pichon, X.; Rangin, C. The North Anatolian Fault. A new look. *Annu. Rev. Earth Planet. Sci.* **2005**, *33*, 37–112. [CrossRef]
12. Di Giacomo, D.; Bondár, I.; Storchak, D.A.; Engdahl, E.R.; Bormann, P.; Harris, J. ISCGEM:Global Instrumental Earthquake Catalogue (1900–2009): III. Re-computed M_S and m_b, proxy M_W, final magnitude composition and completeness assessment. *Phys. Earth Planet. Inter.* **2015**, *239*, 33–47. [CrossRef]
13. Emre, Ö.; Duman, T.Y.; Özalp, S.; Şaroğlu, F.; Olgun, Ş.; Elmacı, H.; Çan, T. Active fault database of Turkey. *Bull. Earthq. Eng.* **2018**, *16*, 3229–3275. [CrossRef]
14. Armijo, R.; Pondard, N.; Meyer, B.; Uçarkus, G.; de Lépinay, B.M.; Malavieille, J.; Dominguez, S.; Gustcher, M.; Schmidt, S.; Beck, C.; et al. Submarine fault scarps in the Sea of Marmara pull-apart (North Anatolian Fault): Implications for seismic hazard in Istanbul. *Geochem. Geophys. Geosyst.* **2005**, *6*, Q06009. [CrossRef]
15. Lorenzo-Martin, F.; Roth, F.; Wang, R.J. Elastic and inelastic triggering of earthquakes in the North Anatolian Fault zone. *Tectonophysics* **2006**, *424*, 271–289. [CrossRef]
16. Pınar, A.; Coşkun, Z.; Mert, A.; Kalafat, D. Frictional strength of North Anatolian fault in eastern Marmara region. *Earth Planets Space* **2016**, *68*, 62. [CrossRef]
17. Barka, A.A. The North Anatolian fault zone. *Ann. Tectonicae* **1992**, *6*, 164–195.
18. Armijo, R.; Meyer, B.; Barka, A.; Chabalier, J.B.; Hubert-Ferrari, A.; Çakir, Z. The fault breaks of the 1999 earthquakes in Turkey and the tectonic evolution of the Sea of Marmara: A summary. In *The 1999 Izmit and Düzce Earthquakes: Preliminary Results*; Barka, A., Kozacı, Ö., Akyüz, S., Altunel, E., Eds.; İstanbul Technical University Press: İstanbul, Turkey, 2000; pp. 55–62.
19. Sesetyan, K.; Demircioglu, M.; Rovida, A.; Albini, P.; Stucchi, M.; Zare, M.; Viganò, D.; Locati, M. SHARE-CET, the SHARE Earthquake Catalogue for Central and Eastern Turkey Complementing the SHARE European Catalogue (SHEEC). 2012. Available online: https://www.emidius.eu/SHEEC/docs/SHARE_CET.pdf (accessed on 1 February 2025).
20. Mantovani, E.; Viti, M.; Babbucci, D.; Albarello, D. Nubia-Eurasia kinematics: An alternative interpretation from Mediterranean and North Atlantic evidence. *Ann. Geophys.* **2007**, *50*, 311–336. [CrossRef]
21. Mantovani, E.; Viti, M.; Babbucci, D.; Tamburelli, C.; Cenni, N.; Baglione, M.; D'Intinosante, V. Generation of back-Arc Basins as Side Effect of Shortening Processes: Examples from the Central Mediterranean. *Int. J. Geosci.* **2014**, *5*, 1062–1079. [CrossRef]
22. Mantovani, E.; Viti, M.; Babbucci, D.; Tamburelli, C.; Cenni, N. Geodynamics of the central-western Mediterranean region: Plausible and non-plausible driving forces. *Marine Petroleum Geology* **2020**, *113*, 104121. [CrossRef]
23. Mantovani, E.; Babbucci, D.; Tamburelli, C.; Viti, M. Late Cenozoic evolution and present tectonic setting of the Aegean–Hellenic Arc. *Geosciences* **2022**, *12*, 104. [CrossRef]
24. Mantovani, E.; Viti, M.; Babbucci, D.; Tamburelli, C.; Hoxha, I.; Piccardi, L. Geodynamics of the South Balkan and Northern Aegean Regions Driven by the Westward Escape of Anatolia. *Int. J. Geosci.* **2023**, *14*, 480–504. [CrossRef]
25. Mantovani, E.; Viti, M.; Babbucci, D.; Tamburelli, C.; Baglione, M.; D'Intinosante, V. Ductile Versus Brittle Tectonics in the Anatolian–Aegean–Balkan System. *Geosciences* **2024**, *14*, 277. [CrossRef]
26. Mantovani, E.; Viti, M.; Babbucci, D.; Tamburelli, C. Plio–Quaternary Tectonic Activity in the Northern Nubian Belts: The Main Driving Forces. *Appl. Sci.* **2025**, *15*, 587. [CrossRef]

27. Mantovani, E.; Viti, M.; Tamburelli, C.; Babbucci, D.; Baglione, M.; D'Intinosante, V. Tectonic Setting and Spatiotemporal Earthquake Distribution in Northern Nubia and Iberia. *Geosciences* **2025**, *15*, 49. [CrossRef]
28. Viti, M.; Mantovani, E.; Tamburelli, C.; Babbucci, D. Generation of trench-arc-backarc systems in the Western Mediterranean region driven by plate convergence. *Ital. J. Geosci.-Boll. Della Soc. Geol. Ital.* **2009**, *128*, 89–106.
29. Viti, M.; Mantovani, E.; Babbucci, D.; Tamburelli, C. Plate kinematics and geodynamics in the Central Mediterranean. *J. Geodyn.* **2011**, *51*, 190–204. [CrossRef]
30. Viti, M.; Mantovani, E.; Babbucci, D.; Tamburelli, C.; Caggiati, M.; Riva, A. Basic role of extrusion processes in the Late Cenozoic of the western and central Mediterranean belts. *Geosciences* **2021**, *11*, 499. [CrossRef]
31. Roussel, J. Les zones actives et la frequence des seismes en Algerie (1716–1970). *Bull. Soc. Hist. Nat. Afr. Nord. Alger* **1973**, *64*, 211–227.
32. Mezcua, J.; Martinez Solares, J.M. *Sismicidad del Area Ibero-Moghrebi. Publicacion 203*; Instituto Geografico Nacional: Madrid, Spain, 1983; p. 302.
33. Benouar, D. Materials for the investigation of the seismicity of Algeria and adjacent regions during the twentieth century. *Ann. Geofis.* **1994**, *37*, 459–860. [CrossRef]
34. Godey, S.; Bossu, R.; Guilbert, J.; Mazet-Roux, G. The Euro-Mediterranean Bulletin: A comprehensive seismological bulletin at regional scale. *Seismol. Res. Lett.* **2006**, *77*, 460–474. [CrossRef]
35. Ekström, G.; Nettles, M.; Dziewonski, A.M. The global CMT project 2004–2010 Centroid-moment tensors for 13,017 earthquakes. *Phys. Earth Planet. Inter.* **2012**, *200–201*, 1–9. [CrossRef]
36. Grünthal, G.; Wahlström, R. The European-Mediterranean Earthquake Catalogue (EMEC) for the last millennium. *J. Seismol.* **2012**, *16*, 535–570. [CrossRef]
37. Makropoulos, K.; Kaviris, G.; Kouskouna, V. An updated and extended earthquake catalogue for Greece and adjacent areas since 1900. *Nat. Hazards Earth Syst. Sci.* **2012**, *12*, 1425–1430. [CrossRef]
38. Stucchi, M.; Rovida, A.; Capera, A.A.G.; Alexandre, P.; Camelbeeck, T.; Demircioglu, M.B.; Gasperini, P.; Kouskouna, V.; Musson, R.M.W.; Radulian, M.; et al. SHARE European earthquake catalogue (SHEEC) 1000–1899. *J. Seismol.* **2012**, *17*, 523–544. [CrossRef]
39. ISIDe Working Group. *Italian Seismological Instrumental and Parametric Database (ISIDe)*; Version 1.0; Istituto Nazionale di Geofisica e Vulcanologia (INGV): Rome, Italy, 2016. [CrossRef]
40. Rovida, A.; Locati, M.; Camassi, R.; Lolli, B.; Gasperini, P.; Antonucci, A. *Italian Parametric Earthquake Catalogue (CPTI15)*; Version 4.0; Istituto Nazionale di Geofisica e Vulcanologia (INGV): Rome, Italy, 2022. [CrossRef]
41. Incorporated Research Institutions for Seismology (IRIS). Available online: http://ds.iris.edu/ieb/ (accessed on 1 February 2025).
42. Kiratzi, A.A. Stress tensor inversions along the westernmost North Anatolian Fault Zone and its continuation into the North Aegean Sea. *Geophys. J. Int.* **2002**, *151*, 360–376. [CrossRef]
43. Sun, Y.-S.; Melgar, D.; Ruiz-Angulo, A.; Ganas, A.; Taymaz, T.; Crowell, B.; Xu, X.; Tsironi, V.; Karasante, I.; Yolsal-Çevikbilen, S.; et al. The 2020 M_w 7.0 Samos (Eastern Aegean Sea) Earthquake: Joint source inversion of multitype data, and tsunami modelling. *Geophys. J. Int.* **2024**, *237*, 1285–1300. [CrossRef]
44. Bozkurt, E. Timing of extension on the Büyük Menderes Graben, western Turkey, and its tectonic implications. In *Tectonics and Magmatism in Turkey and the Surrounding Area*; Bozkurt, E., Winchester, J.A., Piper, J.D.A., Eds.; Geological Society Special Publication no. 173; Geological Society: London, UK, 2000; pp. 385–403.
45. Yılmaz, Y.; Genç, S.C.; Gürer, F.; Bozcu, M.; Yılmaz, K.; Karacik, Z.; Altunkaynak, S.; Elmas, A. When did the western Anatolian grabens begin to develop? In *Tectonics and Magmatism in Turkey and the Surrounding Area*; Bozkurt, E., Bozkurt, J.A., Piper, J.D.A., Winchester, J.A., Eds.; Geological Society of London, Special Publications: London, UK, 2000; Volume 173, pp. 353–384.
46. Çiftçi, N.B.; Bozkurt, E. Evolution of the Miocene sedimentary fill of the Gediz Graben, SW Turkey. *Sediment. Geol.* **2009**, *216*, 49–79. [CrossRef]
47. Sachpazi, M.; Hirn, A.; Clément, C.; Haslinger, F.; Laigle, M.; Kissling, E.; Charvis, P.; Hello, Y.; Lépine, J.-C.; Sapin, M.; et al. Western Hellenic Subduction and Cephalonia Transform: Local Earthquakes and Plate Transport and Strain. *Tectonophysics* **2000**, *319*, 301–319. [CrossRef]
48. Karakostas, V.G.; Papadimitriou, E.E.; Karamanos, C.K.; Kementzetzidou, D.A. Microseismicity and seismotectonic properties of the Lefkada—Kefalonia seismic zone. *Bull. Geol. Soc. Greece* **2010**, *43*, 2053–2063. [CrossRef]
49. Armijo, R.; Meyer, B.; King, G.C.P.; Rigo, A.; Papanastassiou, D. Quaternary evolution of the Corinth rift and its implications for the late Cenozoic evolution of the Aegean. *Geophys. J. Int.* **1996**, *126*, 11–53. [CrossRef]
50. Hatzfeld, D.; Karakostas, V.; Ziazia, M.; Kassaras, I.; Papadimitriou, E.; Makropoulos, K.; Voulgaris, N.; Papaioannou, C. Microseismicity and faulting geometry in the Gulf of Corinth (Greece). *Geophys. J. Int.* **2000**, *141*, 438–456. [CrossRef]
51. Ganas, A.; Drakatos, G.; Pavlides, S.B.; Stavrakakis, G.N.; Ziazia, M.; Sokos, E.; Karastathis, V.K. The 2001 Mw = 6.4 Skyros earthquake, conjugate strike-slip faulting and spatial variation in stress within the central Aegean Sea. *J. Geodyn.* **2005**, *39*, 61–77. [CrossRef]

52. Papadopoulos, G.A.; Agalos, A.; Karavias, A.; Triantafyllou, I.; Parcharidis, I.; Lekkas, E. Seismic and Geodetic Imaging (DInSAR) Investigation of the March 2021 Strong Earthquake Sequence in Thessaly, Central Greece. *Geosciences* **2021**, *11*, 311. [CrossRef]
53. Georgiev, I.; Dimitrov, D.; Belijashki, T.; Pashova, L.; Shanov, S.; Nikolov, G. Geodetic constraints on kinematics of southwestern Butgaria from GPS and levelling data. *Geol. Soc. Lond. Spec. Publ.* **2007**, *291*, 143–157. [CrossRef]
54. Dobrev, N. 3D Monitoring of Active Fault Structures in The Krupnik-Kresna Seismic Zone, SW Bulgaria. *Acta Geodyn. Geomater.* **2011**, *8*, 377–388.
55. Yaltırak, C.; Alpar, B.; Yuce, H. Tectonic Elements Controlling the Evolution of the Gulf of Saros (northeastern Aegean Sea, Turkey). *Tectonophysics* **1998**, *300*, 227–248. [CrossRef]
56. Yaltırak, C.; İşler, E.B.; Aksu, A.E.; Hiscott, R.N. Evolution of the Bababurnu Basin and shelf of the Biga Peninsula: Western extension of the middle strand of the North Anatolian Fault Zone, Northeast Aegean Sea, Turkey. *J. Asian Earth Sci.* **2012**, *57*, 103–119. [CrossRef]
57. Aksoy, M.E.; Meghraoui, M.; Vallée, M.; Çakır, Z. Rupture characteristics of the AD 1912 Mürefte (Ganos) earthquake segment of the North Anatolian fault (western Turkey). *Geology* **2010**, *38*, 991–994. [CrossRef]
58. Kiratzi, A. Source Constraints Using Ground Motion Simulations. *Bull. Geol. Soc. Greece* **2013**, *47*, 1128–1137. [CrossRef]
59. Burchfiel, B.; Nakov, R.; Dumurdzanov, N.; Papanikolaou, D.; Tzankov, T.; Serafimovski, T.; King, R.; Kotzev, V.; Todosov, A.; Nurce, B. Evolution and dynamics of the Cenozoic tectonics of the South Balkan extensional system. *Geosphere* **2008**, *4*, 919–938. [CrossRef]
60. Van Hinsbergen, D.; Schmid, S.M. Map view restoration of Aegean-West Anatolian accretion and extension since the Eocene. *Tectonics* **2012**, *31*, 5. [CrossRef]
61. Piccardi, L.; Dobrev, N.; Moratti, G.; Corti, G.; Tondi, E.; Vannucci, G.; Matova, M.; Spina, V. Overview and New Data on the Active Tectonics of Bulgaria: Towards a Comprehensive Seismotectonic Map. *Acta Volcanol.* **2013**, *25*, 67–82.
62. Finetti, I.R.; Lentini, F.; Carbone, S.; Del Ben, A.; Di Stefano, A.; Forlin, E.; Guarnieri, P.; Pipan, M.; Prizzon, A. Geological Outline of Sicily and Lithospheric Tectono-Dynamics of its Tyrrhenian Margin from New CROP Seismic Data. In *CROP PROJECT, Deep Seismic Exploration of the Central Mediterranean and Italy*; Finetti, I.R., Ed.; Elsevier: Amsterdam, The Netherlands, 2005; Chapter 15; pp. 319–376.
63. Sulli, A.; Morticeli, M.G.; Agate, M.; Zizzo, E. Active north-vergent thrusting in the northern Sicily continental margin in the frame of the Quaternary evolution of the Sicilian collisional system. *Tectonophysics* **2021**, *802*, 228717. [CrossRef]
64. Pondrelli, S.; Salimbeni, S.; Ekström, G.; Morelli, A.; Gasperini, P.; Vannucci, G. The Italian CMT dataset from 1977 to the present. *Phys. Earth Planet. Inter.* **2006**, *159*, 286–303. [CrossRef]
65. Loreto, M.F.; Palmiotto, C.; Muccini, F.; Ferrante, V.; Zitellini, N. Inverted Basins by Africa–Eurasia Convergence at the Southern Back-Arc Tyrrhenian Basin. *Geosciences* **2021**, *11*, 117. [CrossRef]
66. Malinverno, A.; Ryan, W.B.F. Extension in the Tyrrhenian sea and shortening in the Apennines as result of arc migration driven by sinking of the lithosphere. *Tectonics* **1986**, *5*, 227–245. [CrossRef]
67. Royden, L.H. Evolution of retreating subduction boundaries formed during continental collision. *Tectonics* **1993**, *12*, 629–638. [CrossRef]
68. Rosenbaum, G. Geodynamics of oroclinal bending: Insights from the Mediterranean. *J. Geodyn.* **2014**, *82*, 5–15. [CrossRef]
69. Van Hinsbergen, D.J.J.; Vissers, R.L.M.; Spakman, W. Origin and consequences of western Mediterranean subduction, rollback and slab segmentation. *Tectonics* **2014**, *33*, 393–419. [CrossRef]
70. Royden, L.; Faccenna, C. Subduction orogeny and the late Cenozoic evolution of the Mediterranean Arcs. *Annu. Rev. Earth Planet. Sci.* **2018**, *46*, 261–289. [CrossRef]
71. Romagny, A.; Jolivet, L.; Menant, A.; Bessière, E.; Maillard, A.; Canva, A.; Gorini, C.; Augier, R. Detailed tectonic reconstructions of the western Mediterranean region for the last 35 Ma, insights on driving mechanisms. *Bull. Société Géologique Fr.* **2020**, *191*, 37. [CrossRef]
72. Jolivet, L.; Menant, A.; Roche, V.; Le Pourhiet, L.; Maillard, A.; Augier, R.; Do Couto, D.; Gorini, C.; Thinon, I.; Canva, A. Transfer zones in Mediterranean back-arc regions and tear faults. *BSGF Earth Sci. Bull.* **2021**, *192*, 11. [CrossRef]
73. Faccenna, C.; Becker, T.W.; Auer, L.; Billi, A.; Boschi, L.; Brun, J.P.; Capitanio, F.A.; Funiciello, F.; Horvàth, F.; Jolivet, L.; et al. Mantle dynamics in the Mediterranean. *Rev. Geophys.* **2014**, *52*, 283–332. [CrossRef]
74. Feigl, K.L.; Thatcher, W. Geodetic observations of post-seismic transients in the context of the earthquake deformation cycle. *Comptes Rendus Geosci.* **2006**, *338*, 1012–1028. [CrossRef]
75. Hearn, E.H.; McClusky, S.; Ergintav, S.; Reilinger, R.E. Izmit earthquake postseismic deformation and dynamics of the North Anatolian Fault Zone. *J. Geophys. Res.* **2009**, *114*, B08405. [CrossRef]
76. Viti, M.; Mantovani, E.; Cenni, N.; Vannucchi, A. Post Seismic Relaxation: An Example of Earthquake Triggering in the Apennine Belt (1915–1920). *J. Geodyn.* **2012**, *61*, 57–67. [CrossRef]

77. Ergintav, S.; Vernant, P.; Tan, O.; Karabulut, H.; Özarpacı, S.; Floyd, M.; Konca, A.Ö.; Çakır, Z.; Acarel, D.; Çakmak, R.; et al. Unexpected far-field deformation of the 2023 Kahramanmaraş earthquakes revealed by space geodesy. *Science* **2024**, *386*, 328–335. [CrossRef]
78. Mercier, J.L.; Simeakis, K.; Sorel, D.; Vergely, P. Extensional tectonic regimes in the Aegean basins during the Cenozoic. *Basin Res.* **1989**, *2*, 49–71. [CrossRef]
79. Armijo, R.; Lyon-Caen, H.; Papanastassiou, D. East-west extension and Holocene normal-fault scarps in the Hellenic arc. *Geology* **1992**, *20*, 491–494. [CrossRef]
80. Di Bucci, D.; Burrato, P.; Vannoli, P.; Valensise, G. Tectonic evidence for the ongoing Africa-Eurasia convergence in central Mediterranean foreland areas: A journey among long-lived shear zones, large earthquakes, and elusive fault motions. *J. Geophys. Res.* **2010**, *115*, B12404. [CrossRef]
81. Meghraoui, M.; Pondrelli, S. Active faulting and transpression tectonics along the plate boundary in North Africa. *Ann. Geophys.* **2012**, *55*, 5. [CrossRef]
82. Booth-Rea, G.; Gaidi, S.; Melki, F.; Marzougui, W.; Azañón, J.M.; Zargouni, F.; Galvé, J.P.; Pérez-Peña, J.V. Late Miocene extensional collapse of northern Tunisia. *Tectonics* **2018**, *37*, 1626–1647. [CrossRef]
83. Jolivet, L.; Baudin, T.; Calassou, S.; Chevrot, S.; Ford, M.; Issautier, B.; Lasseur, E.; Masini, E.; Manatschal, G.; Mouthereau, F.; et al. Geodynamic evolution of a wide plate boundary in the Western Mediterranean, near-field versus far-field interactions. *BSGF Earth Sci. Bull.* **2021**, *192*, 48. [CrossRef]
84. Mantovani, E.; Viti, M.; Cenni, N.; Babbucci, D.; Tamburelli, C. Present velocity field in the Italian region by GPS data: Geodynamic/tectonic implications. *Int. J. Geosci.* **2015**, *6*, 1285–1316. [CrossRef]
85. Serpelloni, E.; Cavaliere, A.; Martelli, L.; Pintori, F.; Anderlini, L.; Borghi, A.; Randazzo, D.; Bruni, S.; Devoti, R.; Perfetti, P.; et al. Surface velocities and strain-rates in the Euro-Mediterranean region from massive GPS data processing. *Front. Earth Sci.* **2022**, *10*, 907897. [CrossRef]
86. Mantovani, E.; Babbucci, D.; Tamburelli, C.; Viti, M. A review on the driving mechanism of the Tyrrhenian-Apennines system: Implications for the present seismotectonic setting in the Central-Northern Apennines. *Tectonophysics* **2009**, *476*, 22–40. [CrossRef]
87. DeVries, P.M.R.; Krastev, P.G.; Meade, B.J. Geodetically constrained models of viscoelastic stress transfer and earthquake triggering along the North Anatolian fault. *Geochem. Geophys. Geosyst.* **2016**, *17*, 2700–2716. [CrossRef]